Variational Problems and Partial Differential Equations on Implicit Surfaces: The Framework and Examples in Image Processing and Pattern Formation

Marcelo Bertalmío
Electrical and Computer Engineering, University of Minnesota, Minneapolis, MN 55455

and

Li-Tien Cheng
UCLA Mathematics Department, Los Angeles, CA 90095

and

Stanley Osher
UCLA Mathematics Department, Los Angeles, CA 90095

and

Guillermo Sapiro
Corresponding author: Electrical and Computer Engineering, University of Minnesota, Minneapolis, MN 55455
E-mail: guille@ece.umn.edu

A novel framework for solving variational problems and partial differential equations defined on surfaces is introduced in this paper. The key idea is to implicitly represent the surface as the level set of a higher dimensional function, and solve the problem in a fixed Cartesian coordinate system using this new embedding function. When this is combined with the general theory of harmonic maps, we can address such problems as intrinsic regularization of data defined on the surface and pattern generation using the intrinsic surface geometry. We describe the basic technique and present examples in image processing and computer graphics. More precisely, we address the problems of isotropic and anisotropic regularization of images and direction maps defined on the surface and the problem of intrinsic texture synthesis.

Key Words: variational problems, harmonic maps, partial differential equations, level set method, implicit surfaces, image processing, computer graphics, regularization, pattern formation, texture synthesis.

1. INTRODUCTION

In a number of applications, variational problems and partial differential equations need to be solved for data defined on arbitrary manifolds, three dimensional surfaces in particular. Examples of this exist in the areas of mathematical physics, fluid dynamics, image processing, medical imaging, computer graphics, and pattern formation; specific examples will be given later in this paper. These equations are generally solved on triangulated or polygonal surfaces. This involves the tedious discretization of the equations in general polygonal grids, as well as the difficult numerical computation of other quantities like projections onto the discretized surface (when computing gradients and Laplacians for example). In this paper we present a new framework to solve these variational problems and partial differential equations. The three dimensional surface is represented in an implicit form, as the zero level set of a higher dimensional function. All the computations are intrinsic to the surface, but are performed in the Cartesian grid of the higher dimensional embedding. We can then use well studied numerical techniques for solving these equations, and derive simple and elegant implementations.

Representing deforming curves and surfaces as level sets of higher dimensional functions was introduced in [38] as a very efficient technique for numerically studying the deformation. The idea is to represent the surface deformation via the embedding function deformation, migrating from a Lagrangian system (attached to the deforming object) to an Euclidean one. When the velocity of the deformation is given by the Euler-Lagrange of a pre-described variational formulation, the authors in [57] extended the level set ideas to a "variational level set" method (see also [58] for an application of this in surface reconstruction). The basic concept is to transform the variational problem governing the surface deformation into a variational problem defined for the whole embedding function (the whole Euclidean space). The trick for doing this is, in the energy, to penalize only on the level set of interest. This is done via delta functions (in the sense of distributions), see below. The advantage of this approach is that the surface deformation is obtained from the gradient descent of this new variational problem, and can then be implemented in a fixed Cartesian coordinate system. That is, in the variational level set approach, the energy is first re-defined on the embedding, higher dimensional function, and then the gradient descent is computed. For a recent comprehensive review of the level set method see [39].

In this paper we combine the concepts of the variational level set technique with those from areas like harmonic maps. In order to solve a variational problem that is intrinsically defined on a given surface (that is, the data is defined on a surface), we consider the surface as the (zero) level set of a higher dimensional function, and redefine the corresponding variational formulation. We then compute the gradient descent of this energy, and implement it on the natural Cartesian coordinate system. Similarly we proceed for general partial differential equations, not necessarily gradient descent flows (in this case, we just recompute the needed components of

the equation for an implicit representation). Note that in the variational level set framework (as well as in the original level set technique), the surface is deforming. In our case, the surface (and the corresponding higher dimensional embedding function) are fixed, and given by the problem at hand. What is "deforming" is the data defined on the surface. The deformation is given by the corresponding gradient descent flow or PDE.

Before we proceed, it is important to make a number of remarks. Note that in a number of applications, the surfaces are already given in implicit form, e.g., [11], therefore, the framework introduced in this paper is not only simple and robust, it is also natural in those applications. On the other hand, not all surfaces are originally represented in an implicit form. Actually (and unfortunately), triangulated representations, for example, are still much more popular (especially in the computer graphics community). We will then need to apply an algorithm that transforms the given explicit representation into an implicit one. Note of course that this needs to be done only once for each non-implicit surface. Although this is still a very active area of research, many very good algorithms have been developed for this, e.g., [21, 35, 55]. The triangulated surfaces could also be represented in implicit form via polynomials, e.g., [23]. We therefore assume from now on that the three dimensional surface $\mathcal{S}$ of interest is given in implicit form, as the zero level set of a given function $\psi : \mathbb{R}^3 \to \mathbb{R}$. This function is negative inside the closed bounded region defined by $\mathcal{S}$, positive outside, Lipschitz continuous, with $\mathcal{S} \equiv \{x \in \mathbb{R}^3 : \psi(x) = 0\}$. Related to this, it might happen that the data to be processed is only defined on the surface $\mathcal{S}$, hence on the zero level set of ψ. We need then to extend this data in a smooth fashion to be defined for all points $x \in \mathbb{R}^3$ in order to be able to work with ψ and the Cartesian coordinate system. One possibility, inspired by the extension of velocities first suggested and implemented in [14] and then analyzed carefully in [57] for the classical level set technique, is to extend the data u defined on $\mathcal{S}$ (and on the zero level set of ψ) in such a form that it is constant normal to each level set of ψ. This means the extension satisfies $\nabla u \cdot \nabla \psi = 0$. (For simplicity, we assume now u to be a scalar function, although we will also address in this paper problems where the data defined on $\mathcal{S}$ is vector valued. This is solved in an analogous fashion.) To solve this we numerically search for the steady state solution of

$$\frac{\partial u}{\partial t} + \text{sign}(\psi)(\nabla u \cdot \nabla \psi) = 0.$$

Note that this keeps the given data u on the zero level set of ψ (the given surface) unchanged. As a result of this process, the data is now defined on the whole space, and not just on the level set of interest. This data extension needs to be done only once, before the gradient descent or PDE given by the problem is applied. In spite of this, to improve stability and accuracy, we will run this data extension step every few iterations of the PDE (this is analogous to the embedding function re-initialization commonly performed in the classical level set framework). Finally, and also inspired by techniques by now classical in the level set framework, e.g., [40], we will solve the variational problem or PDE only in a band surrounding the zero level set.

The remainder of this paper is organized as follows. In Section 2 we briefly introduce the general theory of harmonic maps. This provides a natural framework for defining variational problems and PDE's on surfaces, and will be used in this paper to exemplify our framework. The general framework is then given in Section 3. Specific examples in image processing, diffusion of direction data, and pattern formation are given in sections 4.1, 4.2, and 4.3 respectively. Section 5 addresses areas of future research opened by this new framework.

2. HARMONIC MAPS

The theory of harmonic maps comprises one of the most studied areas in mathematics. The basic idea is to search for maps u between Riemannian manifolds (M, g) and (N, h) which are critical points (that is, minimizers) of the *p-harmonic energy*

$$E_p(u) = \int_M \| \nabla_M u \|^p \, \mathrm{dvol} M, \tag{1}$$

where $\| \nabla_M u \|$ is the length of the differential in M. The critical points of (1) are called *p-harmonic maps* (or simply *harmonic maps* for $p = 2$). This is in analogy to the critical points of the Dirichlet energy $\int_\Omega \| \nabla f \|^2$ for real valued functions f, which are called *harmonic functions.* For the most popular case of $p = 2$, the Euler-Lagrange equation corresponding to (1) is a simple formula based on Δ_M, the Laplace-Beltrami operator of M, and $A_N(u)$, the second fundamental form of N (assumed to be embedded in $\mathbb{R}^k$) evaluated at u; e.g., [22, 24, 47]:

$$\Delta_M u + A_N(u)\langle \nabla_M u, \nabla_M u \rangle = 0. \tag{2}$$

This leads to a gradient-descent type of flow, that is,

$$\frac{\partial u}{\partial t} = \Delta_M u + A_N(u)\langle \nabla_M u, \nabla_M u \rangle. \tag{3}$$

Particular and important examples of this theory include:

1. $M = \mathbb{R}^2$ and $N = \mathbb{R}$ (with the classical metrics): In this case, $u : \mathbb{R}^2 \to \mathbb{R}$ and we obtain an energy of the form

$$E_p(u) = \int_M \| \nabla u \|^p \, \mathrm{dvol} M, \tag{4}$$

where ∇ stands for the ordinary gradient. For $p = 2$ we obtain

$$\frac{\partial u}{\partial t} = \Delta u, \tag{5}$$

as the gradient descent, where Δ is the Laplacian. That is, we have obtained the classic heat flow, commonly used for isotropic diffusion and/or regularization of data (e.g., [34, 53]). For $p = 1$ we obtain the Total Variation equation [43], whose gradient descent is

$$\frac{\partial u}{\partial t} = \mathrm{div}\left(\frac{\nabla u}{\| \nabla u \|} \right). \tag{6}$$

This gives anisotropic diffusion of u (see also [2, 7, 42]).

2. $M = \mathbb{R}^2$ and $N = S^{n-1}$: This is the classic liquid crystals problem, and was recently introduced in [49] for addressing general image processing and computer graphics problems dealing with directional data (see also [13, 41, 46] for related works). Let then $u(x, y, 0) : \mathbb{R}^2 \to S^{n-1}$ be the original image of directions. That is, this is a collection of vectors from $\mathbb{R}^2$ to $\mathbb{R}^n$ such that their unit norm is equal to one, i.e., $\| u(x, y, 0) \| = 1$, where $\| \cdot \|$ indicates Euclidean length. $u_i(x, y, 0) : \mathbb{R}^2 \to \mathbb{R}$ stand for each one of the n components of $u(x, y, 0)$. Let us define the *component gradient* ∇u_i as

$$\nabla u_i := \frac{\partial u_i}{\partial x}\vec{x} + \frac{\partial u_i}{\partial y}\vec{y}, \tag{7}$$

where $\vec{x}$ and $\vec{y}$ are the unit vectors in the x and y directions respectively. From this,

$$\| \nabla u_i \| = \left(\left(\frac{\partial u_i}{\partial x} \right)^2 + \left(\frac{\partial u_i}{\partial y} \right)^2 \right)^{1/2}, \tag{8}$$

gives the absolute value of the component gradient.

The *component Laplacian* is given by

$$\Delta u_i = \frac{\partial^2 u_i}{\partial x^2} + \frac{\partial^2 u_i}{\partial y^2}. \tag{9}$$

We are also interested in the *absolute value of the image gradient*, given by

$$\| \nabla u \| := \left(\sum_{i=1}^{n} \left(\left(\frac{\partial u_i}{\partial x} \right)^2 + \left(\frac{\partial u_i}{\partial y} \right)^2 \right) \right)^{1/2}. \tag{10}$$

The problem of *harmonic maps in liquid crystals* is then formulated as the search for the solution to

$$\min_{u:\mathbb{R}^2 \to S^{n-1}} \int_\Omega \| \nabla u \|^p \, dxdy, \tag{11}$$

where Ω stands for the data domain and $p \geq 1$. This variational formulation can be re-written as

$$\min_{u:\mathbb{R}^2 \to \mathbb{R}^n} \int_\Omega \| \nabla u \|^p \, dxdy, \tag{12}$$

such that

$$\| u \| = 1. \tag{13}$$

And these reduce to (1) for the selected manifolds.

The corresponding gradient descent flows for $p = 2$ and for general p's are given respectively by (e.g., [49])

$$\frac{\partial u_i}{\partial t} = \Delta u_i + u_i \| \nabla u \|^2, \quad 1 \leq i \leq n, \tag{14}$$

$$\frac{\partial u_i}{\partial t} = \text{div}\left(\| \nabla u \|^{p-2} \nabla u_i \right) + u_i \| \nabla u \|^p, \quad 1 \leq i \leq n. \tag{15}$$

These equations, which can be easily derived from the general gradient descent flow presented above, or by explicit computation of the Euler-Lagrange, define isotropic and anisotropic ($p = 1$) diffusion for directional data defined on the plane.

3. M is a three dimensional surface and $N = \mathbb{R}$: This will be one of the cases studied in this paper. It basically deals with scalar data defined on a surface. The corresponding variational problem is given by (1) and the gradient descent for $p = 2$ is (since the second fundamental form is zero):

$$\frac{\partial u}{\partial t} = \Delta_M u. \tag{16}$$

Note the use of the Laplace-Beltrami operator Δ_M. This leads to isotropic diffusion of data defined on three dimensional surfaces. Similarly we obtain the gradient descent for $p = 1$, anisotropic diffusion.

4. M is a three dimensional surface and $N = S^{n-1}$: Here we obtain directional data defined on a three dimensional surface, and this constitutes an additional example that will be later detailed in this paper. The minimization problem is as in (1) (with the minimizers restricted to be a direction, that is, a unit norm vector), and for $p = 2$ the corresponding gradient descent flow is given by

$$\frac{\partial u_i}{\partial t} = \Delta_M u_i + u_i \| \nabla u \|^2, \quad 1 \leq i \leq n. \tag{17}$$

This leads to isotropic diffusion of vectorial data on three dimensional surfaces (note again the use of the Laplace-Beltrami operator). Similarly, anisotropic diffusion is obtained for $p = 1$.

Before proceeding with the presentation of our framework, which will be exemplified among other cases for the cases in points 3. and 4. above (work onto general three dimensional target surfaces is reported in [36]), we shall make a few remarks on harmonic maps.

The general form of the harmonic energy, normally from a three dimensional surface (M) to the plane (N) with $p = 2$ (the most classical case, e.g., [22, 24]), was successfully used for example in computer graphics to find smooth maps between two given (triangulated) surfaces (again, normally a surface and the complex or real plane); e.g. [3, 20, 28, 56]. In this case, the search is indeed for the critical point, that is, for the harmonic map between the surfaces. This can be done for example via finite elements [3, 28]. The use of the most general form of the p-harmonic maps for problems in image processing and computer graphics, from general non-flat manifolds into general non-flat manifolds, was introduced in [49] (see also [13, 46] for closely related approaches). Particular cases addressed were $M = \mathbb{R}^2$ (the real plane) and $N = S^{n-1}$, with applications in the regularization of optical flow, gradient directions, and chroma. (These cases will be here extended for M a general three dimensional surface.) In this paper, as well as in [49], we are not just interested in the harmonic map, but in the corresponding gradient descent flow, that is, in the process of computing the map via a partial differential equation (the gradient-descent type flow of the harmonic energy (1)). This is partially motivated

by the fact that the basic diffusion equations for multiscale representations and denoising of gray-valued images are obtained as well as gradient descent flows acting on real-valued data; see for example [7, 42, 43]. Isotropic diffusion (linear heat flow) is just the gradient descent of the L_2 norm of the image gradient, while anisotropic diffusion can be interpreted as the gradient descent flow of more robust functions acting on the image gradient. Even more important than this, looking at the gradient-descent flows will help us to show how our framework can be applied not only to solving variational problems for data on three dimensional surfaces but also to general PDE's defined on surfaces.

Since in the cases above we have an energy formulation, it is straightforward to add additional data-dependent constraints on the minimization process, e.g., preservation of the original average; see for example [43] for examples for gray-valued images. In this case we might indeed be interested in the critical point of the modified energy, which can be obtained as the steady-state solution of the corresponding gradient descent flow.

Most of the literature on harmonic maps deals with $p = 2$ in (1) or (11), the linear case. Some more recent results are available for $1 < p < \infty$, $p \neq 2$, [18, 19], and very few results deal with the case $p = 1$ [27]. The papers [22, 24] are an excellent source of information for regular harmonic maps, while [29] contains a comprehensive review of singularities of harmonic maps (check also [47], a classic on harmonic maps). A classical paper for harmonic maps in liquid crystals, that is, the particular case of (11) (or in general, M being a domain in $\mathbb{R}^n$ and $N = S^{n-1}$), is [8]. A review of some of the relevant literature for image processing and computer graphics problems, as well as a large list of corresponding references, can be found in [49].

3. THE GENERAL FRAMEWORK

We will exemplify our framework with the simplest case, given in point 3. in the previous section, for $p = 2$. That is, we have a scalar function u defined on a three dimensional closed surface $\mathcal{S}$ without boundary, $u : \mathcal{S} \to \mathbb{R}$, and we want to find the minimizer of the energy given by

$$\frac{1}{2} \int_{\mathcal{S}} \| \nabla_{\mathcal{S}} u \|^2 \, d\mathcal{S}, \tag{18}$$

whose gradient descent flow is

$$\frac{\partial u}{\partial t} = \Delta_{\mathcal{S}} u. \tag{19}$$

We assume that $\mathcal{S}$ is given as the zero level set of a function $\psi : \mathbb{R}^3 \to \mathbb{R}$, ψ is negative inside the region bounded by $\mathcal{S}$, positive outside with $\mathcal{S} \equiv \{x \in \mathbb{R}^3 : \psi(x) = 0\}$. We proceed now to redefine the above energy and compute its corresponding gradient descent flow. Let $\vec{v}$ be a generic three dimensional vector, and $P_{\vec{v}}$ the operator that projects a given three dimensional vector onto the plane orthogonal to $\vec{v}$:

$$P_{\vec{v}} := I - \frac{\vec{v} \otimes \vec{v}}{\| \vec{v} \|^2} \tag{20}$$

It is then easy to show that the harmonic energy (18) is equivalent to (see for example [45])

$$\frac{1}{2}\int_{\mathcal{S}} \parallel P_{\vec{N}} \nabla u \parallel^2 d\mathcal{S}, \tag{21}$$

where $\vec{N}$ is the normal to the surface $\mathcal{S}$. In other words, $\nabla_{\mathcal{S}} u = P_{\vec{N}} \nabla u$. We now embed this in the function ψ:

$$\begin{aligned} \hat{u} &:= \min_u \frac{1}{2}\int_{\mathcal{S}} \parallel \nabla_{\mathcal{S}} u \parallel^2 d\mathcal{S} \\ &= \min_u \frac{1}{2}\int_{\mathcal{S}} \parallel P_{\vec{N}} \nabla u \parallel^2 d\mathcal{S} \\ &= \min_u \frac{1}{2}\int_{\Omega \in \mathbb{R}^3} \parallel P_{\nabla \psi} \nabla u \parallel^2 \delta(\psi) \parallel \nabla \psi \parallel dx, \end{aligned} \tag{22}$$

where $\delta(\cdot)$ stands for the delta of Dirac, and all the expressions above are considered in the sense of distributions. The last equality includes the embedding, and it is based on the following simple facts:

1. $\nabla \psi \parallel \vec{N}$.
2. $\int_\Omega \delta(\psi) \parallel \nabla \psi \parallel dx = \int_{\mathcal{S}} d\mathcal{S} =$ surface area.

Intuitively, although the energy lives in the full space, the delta function forces the penalty to be effective only on the level set of interest.

We need now to compute the gradient descent of this energy, and we proceed to do this now. Considering

$$E(u) := \frac{1}{2}\int_{\Omega \in \mathbb{R}^3} \parallel P_{\nabla \psi} \nabla u \parallel^2 \delta(\psi) \parallel \nabla \psi \parallel dx,$$

and μ a perturbation of u,

$$\begin{aligned} \frac{d}{dt}|_{t=0} E(u + t\mu) &= \int_\Omega (P_{\nabla\psi}\nabla u \cdot P_{\nabla\psi}\nabla\mu)\delta(\psi) \parallel \nabla\psi \parallel dx \\ &= \int_\Omega \left(P_{\nabla\psi}\nabla u \cdot \left(\nabla\mu - \frac{\nabla\psi \cdot \nabla\mu}{\parallel \nabla\psi \parallel^2} \nabla\psi \right) \right) \delta(\psi) \parallel \nabla\psi \parallel dx \\ &= \int_\Omega (P_{\nabla\psi}\nabla u \cdot \nabla\mu)\delta(\psi) \parallel \nabla\psi \parallel dx \\ &\quad - \int_\Omega (P_{\nabla\psi}\nabla u \cdot \nabla\psi) \frac{\nabla\psi \cdot \nabla\mu}{\parallel \nabla\psi \parallel^2} \delta(\psi) \parallel \nabla\psi \parallel dx \\ &= \int_\Omega (P_{\nabla\psi}\nabla u \cdot \nabla\mu)\delta(\psi) \parallel \nabla\psi \parallel dx \\ &= -\int_\Omega \nabla \cdot (P_{\nabla\psi}\nabla u \delta(\psi) \parallel \nabla\psi \parallel)\mu dx \\ &= -\int_\Omega \nabla \cdot (P_{\nabla\psi}\nabla u \parallel \nabla\psi \parallel)\delta(\psi)\mu dx \\ &\quad - \int_\Omega (P_{\nabla\psi}\nabla u \cdot \nabla\psi)\delta'(\psi) \parallel \nabla\psi \parallel \mu dx \end{aligned}$$

$$= -\int_{\Omega} \nabla \cdot (P_{\nabla\psi} \nabla u \parallel \nabla\psi \parallel) \delta(\psi) \mu dx$$
$$= -\int_{\mathcal{S}\equiv\{\psi=0\}} \frac{1}{\parallel \nabla\psi \parallel} \nabla \cdot (P_{\nabla\psi} \nabla u \parallel \nabla\psi \parallel) \mu d\mathcal{S}.$$

Since the above has to be zero for all μ, we conclude that at the zero level set of ψ,

$$\frac{1}{\parallel \nabla\psi \parallel} \nabla \cdot (P_{\nabla\psi} \nabla u \parallel \nabla\psi \parallel) = 0,$$

and we naturally extend this to the whole domain Ω by consider this to hold on it.[1] We then obtain that the gradient descent for the "implicit harmonic energy" is given by

$$\frac{\partial u}{\partial t} = \frac{1}{\parallel \nabla\psi \parallel} \nabla \cdot (P_{\nabla\psi} \nabla u \parallel \nabla\psi \parallel). \tag{23}$$

Note of course that all the gradients in this expression are defined in the three dimensional Cartesian space, not in the surface $\mathcal{S}$, thereby making the numerical implementation straightforward. This is the beauty of the approach! Basically, for this equation we use a classical scheme of forward differences in time and a succession of forward and backward differences in space. Backward differences are used for the computation of the projected gradient, while forward differences are used for the computation of the divergence. The other equations in this paper are similarly implemented. This follows techniques as those in [43]. Once again, due to the implicit representation, classic numerics are used, avoiding elaborate projections onto discrete surfaces and discretization on general meshes, e.g., [30].

It is easy to show a number of important properties of this equation:

1. For any second embedding function $\phi = \phi(\psi)$, we obtain the same gradient descent flow. Since both ψ and ϕ have to share the zero level set, and we are only interested in the flow around this zero level set, this means that the flow is (locally) independent of the embedding function.[2]

2. If ψ is the signed distance function, a very popular implicit representation of surfaces, the gradient descent simplifies to

$$\frac{\partial u}{\partial t} = \nabla \cdot (P_{\nabla\psi} \nabla u). \tag{24}$$

3. The expression $\frac{1}{\parallel\nabla\psi\parallel} \nabla \cdot (P_{\nabla\psi} \nabla u \parallel \nabla\psi \parallel)$ is equal to the Laplace-Beltrami $\Delta_{\mathcal{S}}$ of a surface represented in implicit form (see for example [45] for the formula for this Laplace-Beltrami). We could also derive (23) directly from the harmonic maps

[1] We have assumed that $\parallel \nabla\psi \parallel \neq 0$, at least on a band surrounding the zero level set. This assumption is valid since we can make the embedding function to be a distance function ($\parallel \nabla\psi \parallel = 1$), or simply multiply ψ by another function that guarantees that the zero-level set $\mathcal{S}$ is preserved and that the gradient of the new embedding function is not zero. Note that although generating an accurate distance function for a given surface might be a costly procedure, it needs to be done only once for each non-implicit surface.

[2] We thank F. Mémoli for helping with this fact.

flow

$$\frac{\partial u}{\partial t} = \Delta_{\mathcal{S}} u,$$

via the simple geometry exercise of computing $\Delta_{\mathcal{S}} u$ for $\mathcal{S}$ in implicit form.

This last property is of particular significance. It basically shows how to solve general PDE's, not necessarily gradient-descent flows, for data defined on implicit surfaces. All that we need to do is to recompute the components of the PDE for implicit representations of the surface. Note that in this way, conceptually, we can re-define classical planar PDE's on intrinsic surfaces.

Similarly, we obtain the corresponding gradient-descent flows for scalar data on $\psi = 0$ for $p = 1$ (anisotropic flow):

$$\frac{\partial u}{\partial t} = \frac{1}{\| \nabla \psi \|} \nabla \cdot \left(\frac{P_{\nabla \psi} \nabla u}{\| P_{\nabla \psi} \nabla u \|} \| \nabla \psi \| \right), \tag{25}$$

and the equations for unit vectors defined on $\psi = 0$ (maps from $\mathcal{S}$ to S^{n-1})

$$\frac{\partial u}{\partial t} = \frac{1}{\| \nabla \psi \|} \nabla \cdot (P_{\nabla \psi} \nabla u \| \nabla \psi \|). + u \| P_{\nabla \psi} \nabla u \|^2, \;\; p = 2, \tag{26}$$

$$\frac{\partial u}{\partial t} = \frac{1}{\| \nabla \psi \|} \nabla \cdot \left(\frac{P_{\nabla \psi} \nabla u}{\| P_{\nabla \psi} \nabla u \|} \| \nabla \psi \| \right) + u \| P_{\nabla \psi} \nabla u \|, \;\; p = 1. \tag{27}$$

Note that basically, in the harmonic maps gradient descent flow (1), the first component is related to the domain manifold, while the second one relates to both the target manifold (second fundamental form) and the domain manifold (norm of the intrinsic gradient). This explains these last two equations. Since we are embedding the domain manifold, only the components related to it change. The case of embedding the target manifold is addressed in [36].

4. EXPERIMENTAL EXAMPLES

We now exemplify the framework just introduced for a number of simple and useful cases. In addition to the particular equations exemplified below, we can use this framework for solving problems such as mean curvature motion of level sets on manifolds [31], segmentation on manifolds following [10], regularized inverse problems [26], and filling-in on manifolds following [4, 5]. General motion of curves on implicit surfaces is studied in [6, 16].

The numerical implementation used is, as we mentioned before, quite simple, and requires a few hundred lines of $C++$ code. The CPU time required for the diffusion examples is of a few seconds on a standard PC (128Mb RAM, 300MHz) under Linux. For the texture synthesis examples, the CPU time ranges from a few minutes to a few hours, depending on the pattern and parameters chosen. All the volumes used contain roughly 64^3 voxels.

4.1. Diffusion of images on surfaces

The use of partial differential equations for image enhancement has become one of the most active research areas in image processing [12]. In particular, diffusion

equations are commonly used for image regularization, denoising, and multiscale representations (representing the image simultaneously at several scales or levels of resolution). This started with the works in [34, 53], where the authors suggested the use of the linear heat flow for this task. That is, given $u : I\!R^2 \to I\!R$, they proposed to use the isotropic diffusion flow (or heat flow) given by

$$\frac{\partial u}{\partial t} = \Delta u,$$

with the original image as initial condition. When the image is defined on the surface, that is, $u : \mathcal{S} \to I\!R$, the equivalent to this equation is

$$\frac{\partial u}{\partial t} = \Delta_{\mathcal{S}} u.$$

This is the first equation we exemplify. Note that this is simply the gradient descent of the harmonic energy for $M = \mathcal{S}$ and $N = R$. Figure 1 shows examples of intrinsic isotropic diffusion, implemented using the implicit technique described in the previous section (see equation (23)). We present examples for three different surfaces, at three different steps of the evolution, and from different angles. This type of flow and its implementation using the general framework here introduced is crucial for regularization of ill-posed problems, e.g., [26].

The heat flow is the gradient descent of $\int \parallel \nabla u \parallel^2 d\Omega$. Similarly, this last flow is, as we have seen, the gradient descent flow of the harmonic energy. Following [43], we can use $p = 1$ to obtain an intrinsic anisotropic diffusion flow. This is given by equation (25), and examples are given in Figure 2. Figure 3 shows an example of adding a constraint to the surface PDE, following [43]. In this case, the variance of the noise is known and this is added to the variational formulation. To the flow (25) we add

$$\lambda(u - u_0),$$

which comes from the Euler-Lagrange when the constraint $\frac{\lambda}{2}\int_{\mathcal{S}}(u - u_0)^2 d\mathcal{S}$ (or $\frac{\lambda}{2}\int_{I\!R^3}(u - u_0)^2\delta(\psi) \parallel \nabla\psi \parallel dx$) is added to the harmonic energy (λ is a parameter and u_0 is the initial noisy image). In the same figure, compare the results obtained when no constraint is imposed.

The same approach, that of anisotropic diffusion with a stopping term, may be used to perform intrinsic *deblurring*, see [16].

In the examples above we have painted images on the surface. In Figure 4 we regularize intrinsic data. In this case, we have selected to regularize the mean curvature of the surface.

We should note that [33] also showed how to regularize images defined on a surface. The author's approach is limited to functions (not generic surfaces) and only applies to level set based motions. The approach is simply to project the deformation of the data on the surface onto a deformation on the plane.

4.2. Diffusion of directional data on surfaces

In [49], the authors introduced the framework of harmonic maps for the regularization of directional data (unit vectors). The framework was described, and experimental results were presented for flat ($I\!R^2$) domains. Here we give examples

for unit vectors defined on surfaces. That is, u are now unit vectors (i.e., in S^2), defined on the surface $\mathcal{S}$ (zero level set of ψ).

First, in [49, 50] the authors proposed to use direction diffusion for color image enhancement. The basic idea is to normalize the RGB vector (a three dimensional vector) to a unit vector representing the chroma, and diffuse this unit vector with the harmonic maps flow. The corresponding magnitude, representing the brightness, is smoothed separately via scalar diffusion flows. That is, we have to regularize a map onto S^2 (the chroma) and another one onto $\mathbb{R}$ (the brightness). This is now extended for a color image defined on the surface $\mathcal{S}$. In the top row of Figure 5 we use the flow (26) to isotropically smooth color artificially painted on a surface, while the brightness is smoothed using (23). This is repeated in the middle row for anisotropic diffusion both of the chroma, equation (27), and of the brightness, equation (25). Note how the color spreads for the isotropic flow and doesn't spread for the anisotropic one (color edges are preserved). In Figure 6 we repeat this for a real color image painted on the surface, where for smoothing the chroma we use the flow (27) with a constraint related to the noise variance, as discussed before. The brightness is left unchanged. [3]

4.3. Pattern formation on surfaces

The use of reaction-diffusion equations for texture synthesis became very popular in computer graphics following the works of Turk [52] and Witkin and Kass [54]. These works follow original ideas by Turing [51], who showed how reaction diffusion equations can be used to generate patterns. The basic idea in these models is to have a number of "chemicals" that diffuse at different rates and that react with each other. The pattern is then synthesized by assigning a brightness value to the concentration of one of the chemicals. The authors in [52, 54] used their equations for planar textures and textures on triangulated surfaces. By using the framework here described, we can simply create textures on (implicit/implicitized) surfaces, without the elaborated schemes developed in those papers. We proceed to present some examples now. We only present simple examples to illustrate an additional application of our framework. Further studies of this application will be reported elsewhere.

Assuming a simple isotropic model with just two chemicals u_1 and u_2, we have

$$\frac{\partial u_1}{\partial t} = F(u_1, u_2) + D_1 \Delta u_1,$$

$$\frac{\partial u_2}{\partial t} = G(u_1, u_2) + D_2 \Delta u_1,$$

where D_1 and D_2 are two constants representing the diffusion rates and F and G are the functions that model the reaction.

[3] We re-normalize at every discrete step of the numerical evolution to address deviations from the unit norm due to numerical errors [17]. We could also extend the framework in [1] and apply it to our equations.

Introducing our framework, if u_1 and u_2 are defined on a surface $\mathcal{S}$ implicitly represented as the zero level set of ψ we have

$$\frac{\partial u_1}{\partial t} = F(u_1, u_2) + D_1 \frac{1}{\| \nabla\psi \|} \nabla \cdot (P_{\nabla\psi} \nabla u_1 \| \nabla\psi \|), \tag{28}$$

$$\frac{\partial u_2}{\partial t} = G(u_1, u_2) + D_2 \frac{1}{\| \nabla\psi \|} \nabla \cdot (P_{\nabla\psi} \nabla u_2 \| \nabla\psi \|). \tag{29}$$

For simple isotropic patterns, Turk [52] selected

$$F(u_1, u_2) = s(16 - u_1 u_2),$$

$$G(u_1, u_2) = s(u_1 u_2 - u_2 - \beta),$$

where s is a constant and β is a random function representing irregularities in the chemical concentration. Examples of this, for implicit surfaces, are given in Figure 7 (the coupled PDE's shown above are run until steady state is achieved). To simulate anisotropic textures, Figure 8, instead of using additional chemicals as in [52], we use anisotropic diffusion, as suggested in [54]. Additional patterns can be obtained with different combinations of the reaction and diffusion parts of the flow.

5. CONCLUDING REMARKS

In this paper, we have introduced a novel framework for solving variational problems and partial differential equations on surfaces. The technique borrows ideas from the level set theory and the theory of harmonic maps. The surface is embedded in a higher dimensional function, and the Euler-Lagrange flow or PDE is solved in the Cartesian coordinate system of this embedding function. The equations are intrinsic to the implicit surface, following the general formulations in harmonic map theory. In addition to presenting the general approach, we have exemplified it with equations arising in image processing and computer graphics.

We believe this new theory opens up a large number of theoretical and practical questions. In the theoretical arena, we need to extend the large amount of results available for harmonic maps (see for example [49] for a review on this) to the "implicit harmonic maps" framework here introduced. We would also like to investigate the effect of perturbations on the surface (zero-level set) on the solutions of the intrinsic PDE. This is crucial to understand the desired accuracy of surface implicitation algorithms. We expect that as with the level set theory (e.g., [15, 25]), these theoretical results will follow after the presentation of the framework in this paper. On the practical side, we are currently addressing other related equations that appear in the mathematical physics, image processing, and computer graphics literature. For example, we are investigating how to extend the use of harmonic maps for texture mapping (and not just texture synthesis). This was done for triangulated surfaces in [3, 20, 28], and we plan to extend this to implicit surfaces via the implicit framework here introduced. We are also interested in investigating threshold dynamics and convolution generated motions [32, 37, 44] for implicit surfaces. Finally, the use of this framework for regularization in inverse problems is of interest as well. These issues will be reported on elsewhere.

ACKNOWLEDGMENT

We thank Facundo Mémoli for interesting conversations during this work. Some of the implicit surfaces used in this paper were provided by Ravi Malladi. This work was partially supported by grants from the Office of Naval Research ONR-N00014-97-1-0509 and ONR-N00014-97-1-0027, the Office of Naval Research Young Investigator Award, the Presidential Early Career Awards for Scientists and Engineers (PECASE), a National Science Foundation CAREER Award, the National Science Foundation Learning and Intelligent Systems Program (LIS), NSF-DMS-9706827, ARO-DAAG-55-98-1-0323 and IIE-Uruguay.

REFERENCES

1. F. Alouges, "An energy decreasing algorithm for harmonic maps," in J.M. Coron *et al.*, Editors, *Nematics*, Nato ASI Series, Kluwer Academic Publishers, Netherlands, pp. 1-13, 1991.
2. L. Alvarez, P. L. Lions, and J. M. Morel, "Image selective smoothing and edge detection by nonlinear diffusion," *SIAM J. Numer. Anal.* **29**, pp. 845-866, 1992.
3. S. Angenent, S. Haker, A. Tannenbaum, and R. Kikinis, "Laplace-Beltrami operator and brain flattening," *University of Minnesota ECE Report*, Summer 1998.
4. C. Ballester, M. Bertalmío, V. Caselles, G. Sapiro, and J. Verdera, "Filling-in by joint interpolation of vector fields and grey levels," *IMA Technical Report*, University of Minnesota, May 2000.
5. M. Bertalmío, G. Sapiro, V. Caselles, and C. Ballester, "Image inpainting," *SIGGRAPH 2000*, New Orleans, July 2000.
6. M. Bertalmío, G. Sapiro, and G. Randall, "Region tracking on level set methods," *IEEE Trans. Medical Imaging* **18**, pp. 448-451, 1999.
7. M. Black, G. Sapiro, D. Marimont, and D. Heeger, "Robust anisotropic diffusion," *IEEE Trans. Image Processing* **7:3**, pp. 421-432, 1998.
8. H. Brezis, J. M. Coron, and E. H. Lieb, "Harmonic maps with defects," *Communications in Mathematical Physics* **107**, pp. 649-705, 1986.
9. B. Cabral and C. Leedom. "Imaging vector fields using line integral convolution," *ACM Computer Graphics (SIGGRAPH '93)* **27:4**, pp. 263-272, 1993.
10. V. Caselles, R. Kimmel, and G. Sapiro, "Geodesic active contours," *International Journal of Computer Vision* **22:1**, pp. 61-79, 1997.
11. V. Caselles, R. Kimmel, G. Sapiro, and C. Sbert, "Minimal surfaces based object segmentation," *IEEE-PAMI*, **19:4**, pp. 394-398, April 1997.
12. V. Caselles, J. M. Morel, G. Sapiro, and A. Tannenbaum, Editors, "Special Issue on Partial Differential Equations and Geometry-Driven Diffusion in Image Processing and Analysis," *IEEE Trans. Image Processing* **7**, March 1998.
13. T. Chan and J. Shen, "Variational restoration of non-flat image features: Models and algorithms," *UCLA CAM-TR 99-20*, June 1999.
14. S. Chen, B. Merriman, S. Osher, and P. Smereka, "A simple level set method for solving Stefan problems," *Journal of Computational Physics* **135**, pp. 8, 1995.
15. Y. G. Chen, Y. Giga, and S. Goto, "Uniqueness and existence of viscosity solutions of generalized mean curvature flow equations," *J. Diff. Geom.* **33**, 1991.
16. L. T. Cheng, *The Level Set Method Applied to Geometrically Based Motion, Material Science, and Image Processing*, *PhD Thesis Dissertation, UCLA*, June 2000.
17. R. Cohen, R. M. Hardt, D. Kinderlehrer, S. Y. Lin, and M. Luskin, "Minimum energy configurations for liquid crystals: Computational results," in J. L. Ericksen and D. Kinderlehrer, Editors, *Theory and Applications of Liquid Crystals*, pp. 99-121, IMA Volumes in Mathematics and its Applications, Springer-Verlag, New York, 1987.
18. Y. Chen, M.C. Hong and N. Hungerbuhler, "Heat flow of p-harmonic maps with values into spheres," *Math. Z.* **205**, pp. 25-35, 1994.
19. J. M. Coron and R. Gulliver, "Minimizing p-harmonic maps into spheres," *J. Reine Angew. Mathem.* **401**, pp. 82-100, 1989.
20. M. Eck, T. DeRose, T. Duchamp, H. Hoppe, M. Lounsbery, and W. Stuetzle. "Multi-resolution analysis of arbitrary meshes," *Computer Graphics (SIGGRAPH '95 Proceedings)*, pp. 173-182, 1995.

21. M. Eck and H. Hoppe, "Automatic reconstruction of B-spline surfaces of arbitrary topological type," *Computer Graphics*, 1996.

22. J. Eells and L. Lemarie, "A report on harmonic maps," *Bull. London Math. Soc.* **10:1**, pp. 1-68, 1978.

23. G. Taubin, "Estimation of planar curves, surfaces, and nonplanar space curves defined by implicit equations with applications to edge and range image segmentation," *IEEE Trans. PAMI* **13:11**, pp. 1115-1138, 1991.

24. J. Eells and L. Lemarie, "Another report on harmonic maps," *Bull. London Math. Soc.* **20:5**, pp. 385-524, 1988.

25. L. C. Evans and J. Spruck, "Motion of level sets by mean curvature, I," *J. Differential Geometry* **33**, pp. 635-681, 1991.

26. O. Faugeras, F. Clément, R. Deriche, R. Keriven, T. Papadopoulo, J. Gomes, G. Hermosillo, P. Kornprobst, D. Lingrad, J. Roberts, T. Viéville, F. Devernay, "The inverse EEG and MEG problems: The adjoint state approach I: The continuous case," *Inria Research Report* **3673**, June 1999.

27. M. Giaquinta, G. Modica, and J. Soucek, "Variational problems for maps of bounded variation with values in S^1," *Cal. Var.* **1**, pp. 87-121, 1993.

28. S. Haker, S. Angenent, A. Tannenbaum, R. Kikinis, G. Sapiro, and M. Halle, "Conformal surface parameterization for texture mapping," *University of Minnesota IMA Preprint Series* **1611**, April 1999.

29. R. M. Hardt, "Singularities of harmonic maps," *Bulletin of the American Mathematical Society* **34:1**, pp. 15-34, 1997.

30. G. Huiskamp, "Difference formulas for the surface Laplacian on a triangulated surface," *Journal of Computational Physics* **95**, pp. 477-496, 1991.

31. T. Ilmanen, "Generalized flows of sets by mean curvature on a manifold," *Indiana Journal of Math.* **4**, pp. 671-705, 1992.

32. H. Ishii, "A generalization of Bence, Merriman, and Osher algorithm for motion by mean curvature," In A. Damlamian, J. Spruck, and A. Visintin, Editors, *Curvature Flows and Related Topics*, pp. 111-127, Gakkôtosho, Tokyo, 1995.

33. R. Kimmel, "Intrinsic scale space for images on surfaces: The geodesic curvature flow," *Graphical Models and Image Processing* **59**, pp. 365-372, 1997.

34. J. J. Koenderink, "The structure of images," *Biological Cybernetics* **50**, pp. 363-370, 1984.

35. V. Krishnamurthy and M. Levoy, "Fitting smooth surfaces to dense polygon meshes," *Computer Graphics*, pp. 313-324, 1996.

36. F. Mémoli, G. Sapiro, and S. Osher, "Harmonic maps and PDE's onto arbitrary target surfaces," in preparation.

37. B. Merriman, J. Bence, and S. Osher, "Diffusion generated motion by mean curvature," in J. E. Taylor, Editor, *Computational Crystal Growers Workshop*, pp. 73-83, American Mathematical Society, Providence, Rhode Island, 1992.

38. S. J. Osher and J. A. Sethian, "Fronts propagation with curvature dependent speed: Algorithms based on Hamilton-Jacobi formulations," *Journal of Computational Physics* **79**, pp. 12-49, 1988.

39. S. J. Osher and R. P. Fedkiw, "Level set methods," *ULCA CAM Report* **00-07**, February 2000, submitted to *Journal of Computational Physics* **79**.

40. D. Peng, B. Merriman, S. Osher, H. Zhao, M. Kang, "A PDE-based fast local level set method," *Journal of Computational Physics* **155**, pp. 410-438, 1999.

41. P. Perona, "Orientation diffusion," *IEEE Trans. Image Processing* **7**, pp. 457-467, 1998.

42. P. Perona and J. Malik, "Scale-space and edge detection using anisotropic diffusion," *IEEE Trans. Pattern. Anal. Machine Intell.* **12**, pp. 629-639, 1990.

43. L. I. Rudin, S. Osher, and E. Fatemi, "Nonlinear total variation based noise removal algorithms," *Physica D* **60**, pp. 259-268, 1992.

44. S. J. Ruuth, B. Merriman, and S. Osher, "Convolution generated motion as a link between cellular automata and continuum pattern dynamics," *J. of Computational Physics* **151**, pp. 836-861, 1999.

45. L. Simon, *Lectures on Geometric Measure Theory*, Australian National University, Australia, 1984.

46. N. Sochen, R. Kimmel, and R, Malladi, "A general framework for low level vision," *IEEE Trans. Image Processing* **7**, pp. 310-318, 1998.

47. M. Struwe, "On the evolution of harmonic mappings of Riemannian surfaces," *Comment. Math. Helvetici* **60**, pp. 558-581, 1985.

48. M. Struwe, Variational Methods, Springer Verlag, New York, 1990.

49. B. Tang, G. Sapiro, and V. Caselles, "Diffusion of general data on non-flat manifolds via harmonic maps theory: The direction diffusion case," *Int. Journal Computer Vision* **36:2**, pp. 149-161, February 2000.

50. B. Tang, G. Sapiro, and V. Caselles, "Chromaticity diffusion," pre-print, March 1999. Also in *Proc. IEEE Trans. ICIP*, Vancouver, September 2000.

51. A. Turing, "The chemical basis of morphogenesis," *Philosophical Transactions of the Royal Society B* **237**, pp. 37-72, 1952.

52. G. Turk, "Generating textures on arbitrary surfaces using reaction-diffusion," *Computer Graphics* **25:4**, pp. 289-298, , July 1991.

53. A. P. Witkin, "Scale-space filtering," *Int. Joint. Conf. Artificial Intelligence* **2**, pp. 1019-1021, 1983.

54. A.Witkin and M.Kass, "Reaction-diffusion textures," *Computer Graphics* **25:3**, July 1991.

55. G. Yngve and G. Turk, "Creating smooth implicit surfaces from polygonal meshes," *Technical Report GIT-GVU-99-42, Graphics, Visualization, and Usability Center. Georgia Institute of Technology*, 1999.

56. D. Zhang and M. Hebert, "Harmonic maps and their applications in surface matching," *Proc. CVPR '99*, Colorado, June 1999.

57. H. K. Zhao, T. Chan, B. Merriman, and S. Osher, "A variational level set approach to multiphase motion," *J. of Computational Physics* **127**, pp. 179-195, 1996.

58. H. Zhao, S. Osher, B. Merriman, and M. Kang, "Implicit, non-parametric shape reconstruction from unorganized points using a variational level set method," *UCLA CAM Report* **98-7**, February 1998, submitted to *Computer Vision and Image Understanding*.

FIG. 1. Intrinsic isotropic diffusion (from left to right, original followed by two diffusion steps). Top: gray-scale image on a sphere. Middle: gray-scale image on the surface of a head. Bottom: synthetic scalar data on a torus.

FIG. 2. Intrinsic anisotropic diffusion (from left to right). Top: gray-scale image on a sphere. Middle: gray-scale image on the surface of a head. Bottom: synthetic scalar data on a torus.

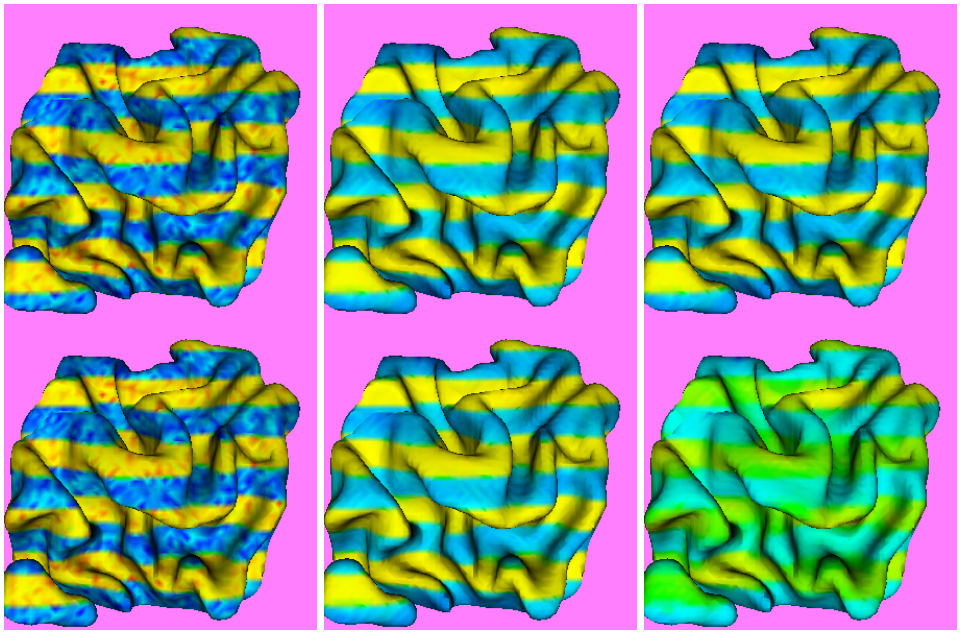

FIG. 3. Intrinsic Total Variation (TV) denoising (anisotropic diffusion with stopping term). Scalar data shown in color for visualization purposes. Top: TV at steps 0 (left), 20 (middle) and 80. Bottom: intrinsic anisotropic diffusion, with no stopping term, also at steps 0, 20 and 80. Notice how TV does not smear the data.

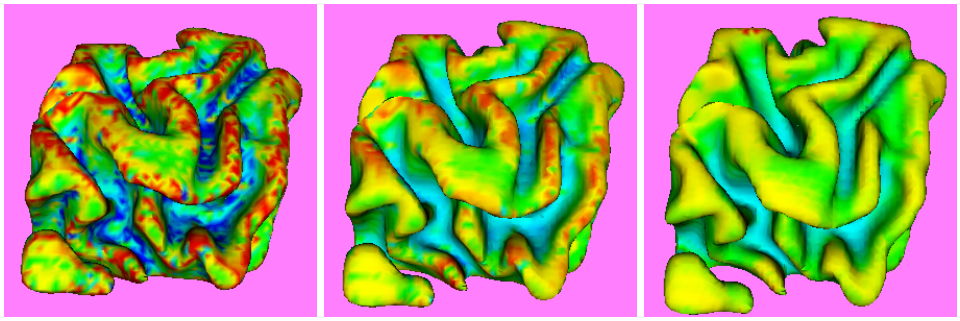

FIG. 4. Anisotropic diffusion of intrinsic data. Mean curvature scalar data (shown in color for visualization purposes) on a MRI section of the visual cortex.

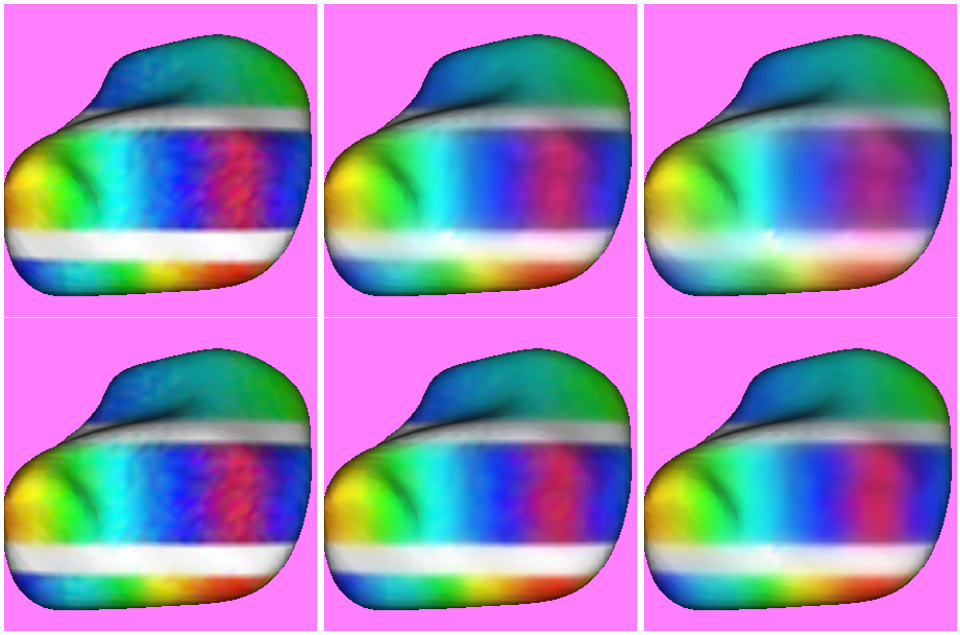

FIG. 5. Diffusion of color images. Top: chroma vectors and brightness values are regularized with isotropic diffusion. Bottom: chroma vectors and brightness values are regularized with anisotropic diffusion.

FIG. 6. Total Variation of chroma vectors, the brightness is left unchanged.

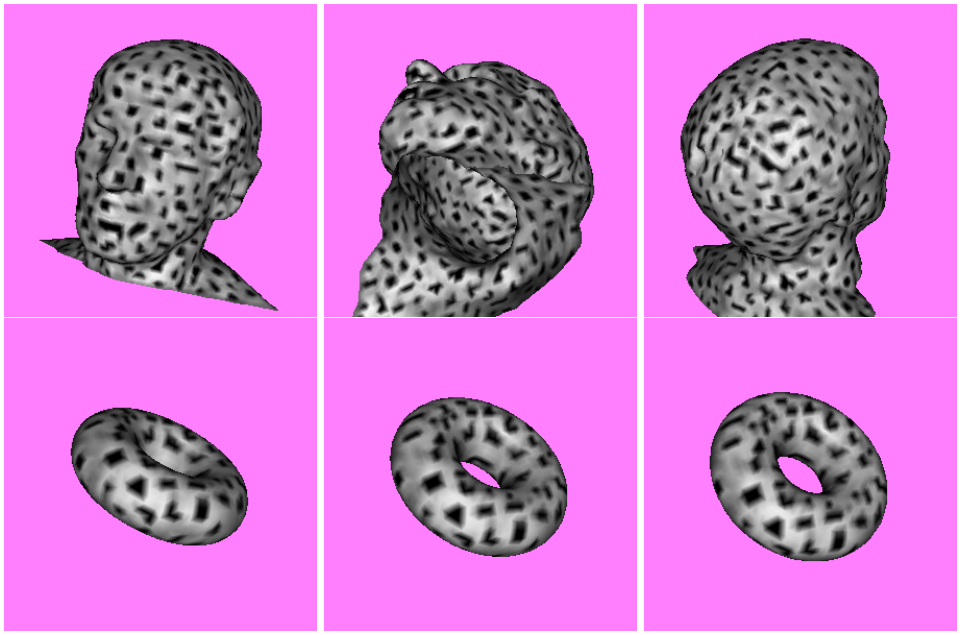

FIG. 7. Intrinsic pattern formation. For each surface, three views are shown.

FIG. 8. Intrinsic pattern formation. Anisotropic patterns are generated using anisotropic diffusion. Three views are shown.